Comparative study of different Bridge Fault Current Limiters applied in Doubly Fed Induction Generator for Improvement of Fault Ride-Through Capability

Afroz Mokarim
Department of Electrical Engineering, Institute of Engineering and Technology
Lucknow, India.
mokarimafroz@gmail.com

Bharti Dwivedi
Department of Electrical Engineering, Institute of Engineering and Technology
Lucknow, India
bharti.dwivedi@ietlucknow.ac.in

Preeti Verma
Department of Electrical Engineering, Institute of Engineering and Technology
Lucknow, India.
preetverma08@gmail.com

***Abstract*—The behavior of a grid-connected Doubly Fed Induction Generator following the occurrence of a fault in the grid has become quite significant from the stable operating point of view. The need for maintaining grid voltage at the time of faults has become very important and the same can be said for the reactive power compensation to the system after the fault clearance. This has necessitated the formation of new grid codes comprising of Low Voltage Ride-Through as one of the major requirements for the integration of wind farms to the grid. The wind farm model is represented by an equivalent array of DFIGs. Temporary Three-Line-To-Ground (3LG) fault was applied to one of the double circuit transmission lines of the test system to investigate the LVRT. In this paper, a study has been carried out to compare the performance of DFIG with and without a Fault Current Limiter (FCL). Further, the performances of Inductive-Resistive Type Bridge Fault Current Limiter (LR-BFCL) and Capacitive-Resistive Type Bridge Fault Current Limiter (CR-BFCL) have been compared. CR-BFCL has been found to give better Fault Ride Through which can be attributed to reactive power injection by it during fault clearance. MATLAB/Simulink environment is used to carry out simulations. The graphical results obtained from simulations show that the CR-BFCL effectively provides reactive power compensation besides improving the Fault Ride Through capability.**

Keywords*— *Doubly Fed Induction Generator (DFIG), Bridge Fault Current Limiter (BFCL), Fault Ride-Through (FRT)

I. Introduction

The last decade has been a witness to many environmental issues and inadequate fossil fuel resources. So, to bring down the environmental impacts of traditional power generation, harnessing renewable energy resources has become the primary objective of the power sector. This can not only reduce carbon emissions but also relieve mankind from the effects of diminishing fossil fuels. Hence, the focus of power systems has been shifted to renewable energy resources and out of all wind energy stands to prove the most worthwhile because of its numerous advantages, like high generation capability, low maintenance, good efficiency, and great abundance. Worldwide wind power was recorded above 50 GW in 2017. To be specific, the total capacity of all installations was 52,492 MW, bringing the global total to 539,123 MW [1]. Various studies have been conducted to obtain smooth power from wind generation systems using power electronics [2-3].

With the increase in the amount of installed Wind Energy Conversion Systems (WECS), it is ever more important that whenever the power system suffers transient disturbances, the turbine generators stay connected to the transmission network in order to ensure grid stability. This special requirement which has been given in the “grid codes” is called Fault Ride-Through (FRT) capability. It specifies that the wind turbines should support the power system operation instead of tripping off during transmission faults. This special requirement which has been given in the “grid codes” is called Fault Ride-Through (FRT) capability. FRT is basically categorized into Low Voltage Ride-Through (LVRT), Zero Voltage Ride-Through (ZVRT) and High Voltage Ride-Through (HVRT) [4]. DFIGs are quite vulnerable to voltage sags because the stator winding is directly connected to the grid and the partial capacities of Rotor Side Converter (RSC) and Grid Side Converter (GSC). These voltage sags at Point of Common Coupling (PCC) result in high rotor currents during faults which may cause the RSC to get damaged. In the LVRT profile, the grid voltage becomes 15% - 25% of its nominal value [5] during grid faults. Hence, LVRT is a major factor of concern for the integration of wind farms to grid. Besides, another requisite to promote fast grid-recovery after fault clearance is to provide reactive power support at the PCC. There are basically two kinds of strategies utilized for the FRT capability improvement given in the literature: external hardware circuits and internal control modifications for DFIG. Many FRT solutions have been proposed in the literature like crowbar protection circuits [6-9]. Addition of crowbar bypasses RSC during faults to protect it from high rotor currents. This, in turn, converts DFIG operation into that of Squirrel Cage Induction Generator (SCIG) causing it to extract reactive power from the PCC. Series Dynamic Breaking Resistor (SDBR) was introduced in [10] showing the effect of elevating the voltage during a fault. Some of the energy storage-based devices like Flywheel Energy Storage (FES) [11] and Superconducting Magnetic Energy Storage (SMES) [12] were also added to the list for the protection of DC-link. To improve the reactive power injection reactive VAR compensators (Static Synchronous Compensator (STATCOM) [13]), Unified Power Flow Controller (UPFC) are proposed in [14].

However, storage based, and VAR compensating devices need extra controllers and are costly. Different control strategies like flux linkage tracking [15], sliding mode control [16], and robust control [17] were also proposed but they needed tuning of different control parameters of the system. It is reported in [18] that for a given MVA rating, the voltage profile at the PCC is better improved by series compensating devices rather than the shunt compensating devices. Therefore, in order to improve the transient stability series devices are gaining more popularity in DFIG based wind generation. The emerging technology of Fault Current Limiters (FCLs) provides a new FRT solution to grid-connected wind farms [19-21]. The application of FCLs in the grid is relevant in supporting the operation of existing devices when fault currents reach very high magnitudes and continue for longer durations. FCL is an innovative device that overcomes the effects of these high fault currents and brings their magnitudes to levels that can be handled by the power system protection equipment. Hence, FCL is effectively capable of improving the FRT performance of wind farms during faults. In [22-24] High-Temperature Superconducting FCL (HT-SFCL) is proposed in different situations to improve the LVRT performance of DFIG based wind farms. In [25], the combination of HT-SFCL and DVR is introduced to boost the voltage profile of wind turbines. The application of the Bridge-Type FCL (BFCL) formed using Superconducting Coil (SC) is proposed in [26] whereas in [27], a DC reactor has been used instead of the SC with an added discharging reactor in the BFCL structure. With this background, it has been established that BFCL consists of a bridge path and an impedance path where the latter introduces high impedance to limit the fault current. Formerly, the structure of BFCL was integrated with an inductive-resistive branch in its impedance path which would increase the LVRT operation of the wind farm. However, in this paper, the impedance path is replaced using a capacitive-resistive branch (namely CR-BFCL) which not only improves the LVRT operation but also supports the reactive power compensation after the fault clearance. To evaluate the proficiency of CR-BFCL, its performance has been paralleled to that of LR-BFCL or simply BFCL. MATLAB/ Simulink software is employed for conducting the respective simulations. A double circuit transmission line power system integrated with DFIG based wind farm is used as the test system.

II. Description of the Test System Model

The simplified model of the power system used for simulations in this work is shown in Fig. 1. It consists of a 20MW DFIG based wind farm that delivers power to the grid through the transformer and a double circuit transmission line. To protect the wind farm from external faults the protective device is positioned in between the wind farm and one of the transmission lines. In reality, these types of wind farms are formed using a number of turbine generator systems which is represented in the model by designing the farm from ten individual wind turbines each having 2 MW as their rated outputs. The parameters of the grid are given in Table 1. This type of organization of wind farm is considered because it depicts more dynamics as compared to the one with a single wind turbine. The parameters of DFIG are given in Table I in the appendix.

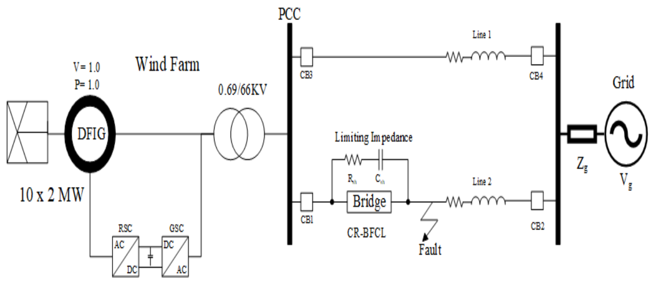

Fig. 1. Test system with DFIG based wind farm

III. Wind Farm Modelling

The wind farm is basically represented by an equivalent turbine and generator system and hence, wind farm modeling comprises of the modeling of both the systems. In addition to the wind turbine and the induction generator, it consists of the grid side converter, the rotor side converter and the DC link.

A. *Aerodynamic Modeling of Wind Turbine*

Various physical and geometrical aspects govern the modeling of the wind turbine. For simplicity, only the electrical behavior of the system is considered which shows that the mechanical power extracted from the kinetic energy of the wind is [28]:

$$P_w = \frac{1}{2}\pi\rho R^2 V^3 C_p\,(\lambda,\beta) \tag{1}$$

Where P_w is the extracted power from the wind, ρ is the air density, R is the blade radius, V is the wind velocity, and C_p is the power coefficient which is a function of both the tip speed ratio λ and the blade pitch angle β and given by:

$$C_p\,(\lambda,\beta) = c_1\left(\frac{c_2}{\lambda_i} - c_3\beta - c_4\right) e^{\frac{-c_5}{\lambda_i}} - c_6\lambda \tag{2}$$

Where,

$$\lambda_i = \left(\frac{1}{\lambda+0.08\beta} - \frac{0.035}{\beta^3+1}\right)^{-1} \tag{3}$$

$c_1 = 0.5176$, $c_2 = 116$, $c_3 = 0.4$, $c_4 = 5$, $c_5 = 21$ and $c_6 = -0.0068$

$$\lambda = \frac{\omega_r R}{V_w} \tag{4}$$

B. *DFIG Modeling*

The DFIG is basically a wound rotor induction generator where the rotor is also fed through a three-phase supply. The equations for stator and rotor in the stationary a-b-c reference frame are given as:

$$V_{ns} = R_s i_{ns} + \frac{d\lambda_{ns}}{dt} \tag{5}$$

$$V_{nr} = R_r i_{nr} + \frac{d\lambda_{nr}}{dt} \tag{6}$$

Where,

$$\lambda_{ns} = L_s i_{ns} + L_m i_{nr} \tag{7}$$

$$\lambda_{nr} = L_r i_{nr} + L_m i_{ns} \tag{8}$$

n= the respective a, b or c phase.

The Park's transformation model [29] was used to model the DFIG, as it converts the three-phase quantities into d-q components facilitating decoupled controllability of real and reactive power.

C. *DFIG Control System*

In designing the control system for the DFIG, Stator Flux Orientation (SFO) method is implemented in which the stator flux is assumed to be aligned with the d-axis of the arbitrary d-q reference frame that rotates synchronously. The electromagnetic torque and the stator reactive power are controlled independently by achieving a decoupled control between the electrical torque and the rotor excitation current.

The work of the RSC controller is to regulate the stator active power through the rotor current q-axis component (I_{qr}) during steady-state operation. The amount of the reactive power exchange that takes place between the stator and the grid through the rotor current d-axis component (I_{dr}) is also controlled by RSC.

The GSC controller has to keep the dc-link voltage constant irrespective of the direction in which the rotor power flows. For this purpose, a vector control approach is employed where the reference frame is oriented along the supply or stator voltage vector position. In this technique, all quantities of voltage and current are converted to a reference frame that rotates with the speed of the supply voltage. To keep the dc-link voltage constant the d-axis component of the current is controlled while the q-axis component is employed to normalize the reactive power flow between the supply and the supply side converter. For this to get implemented, the real axis (d-axis) of the reference frame is kept aligned to the supply voltage vector.

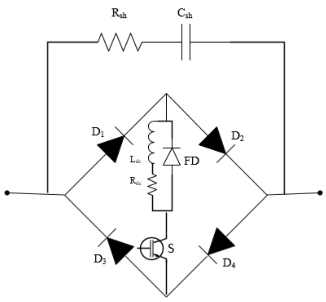

Fig. 2. Schematic diagram of CR-BFCL

IV. Capacitive-Resistive Type BFCL (CR-BFCL)

Fig. 2 shows the per-phase schematic diagram of CR-BFCL showing its simplified circuit. The modeling of CR-BFCL is given in the following subsections. It also shows the operation of CR-BFCL in normal operation and fault conditions.

A. CR-BFCL Configuration

The structure of CR-BFCL consists of two main segments namely the bridge segment and the limiting impedance segment. The bridge segment is made up of four diodes D_1, D_2, D_3, and D_4 connected in bridge formation. One IGBT switch S which is connected in series with a DC reactor is located in the middle of the bridge. The DC reactor is modeled using resistance R_{dc} and inductance L_{dc} along with a freewheeling diode (FD) connected in parallel. The limiting impedance segment is in shunt with the bridge segment and consists of a capacitive-resistive branch modeled as R_{lim} and C_{lim}. The CR-BFCL is designed in accordance with the system criteria and connected in series with the transmission line.

B. CR-BFCL Operation during Normal Conditions

During normal operating conditions the IGBT switch (S) remains closed and the entire line current flows through the diode bridge path. For the positive half cycle of electrical frequency, the line current flows through D_1-R_{dc}-L_{dc}-S-D_4 path whereas for the negative half cycle it flows through D_2-R_{dc}-L_{dc}-S-D_3. The action of bridge circuit results in the conversion of line current from AC to DC and it flows through dc reactor in one direction only. In a couple of cycles, the CR-BFCL enters into the steady-state operation as the L_{dc} in the aforementioned DC reactor is charged and reaches the peak value of the line current. The voltage drop caused due to R_{dc} and IGBT turn-on resistance is negligible compared to the line drop and keeps the dc reactor current constant as i_{dc}. Hence, the bridge causes a negligible impact on the steady-state operation of the system. The shunt path limiting impedance is comparatively large and hence only small leakage current flows through it making almost the whole line current flow through the bridge during normal operation.

C. CR-BFCL Operation during Fault

In the case of a fault, the line current passing through the dc reactor suddenly increases to large magnitudes. When this current i_{dc} reaches above a predefined threshold value i_t, the CR-BFCL control action takes place and generates a low magnitude IGBT gate signal to turn it off. As soon as the IGBT is turned off, the line current previously flowing through the bridge is bypassed to the limiting impedance path. Here, the line current is limited and the excess energy it carries is consumed by the large impedance offered to it. Therefore, the operation of DFIG is safely maintained and its FRT performance is improved. The energy stored in the dc reactor is discharged through the freewheeling diode (FD) and hence IGBT is saved from high switching current during its turn on.

After fault clearance, the voltage at PCC starts restoring back to the pre-fault value. The system begins to recover after circuit breakers have opened and the faulty line has been isolated. Again, as soon as the voltage at PCC attains some specific threshold value V_{th}, the IGBT switch turns on and the system returns to the normal operational condition. The strategy used to control the operation of CR-BFCL is shown in Fig. 3. The RMS voltage and line current at PCC are measured and compared with their respective threshold values to turn on and turn off the IGBT.

D. CR-BFCL Design Considerations

The dc reactor is designed in a way that it controls the incremental rise of the short circuit current at fault instant. To design the values of capacitive-resistive impedance branch we have to consider the effects of C_{lim} and R_{lim} in the system.

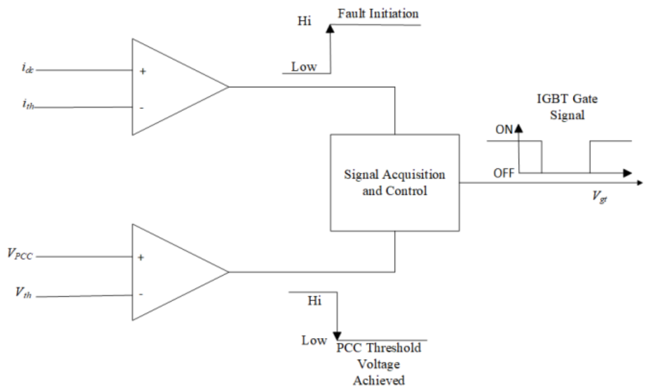

Fig. 3. Control Strategy for switching of CR-BFCL

In the process of limiting the fault current, R_{lim} dissipates the excess amount of electrical energy from the system during fault and hence, prevents the DFIG rotor from acceleration. C_{lim}, on the other hand, provides reactive power support to the DFIG after fault clearance. This helps in fast grid recovery and improves the voltage profile. During normal operation, each line of the double circuit transmission line equally carries half of the amount of active power generated by DFIG (P).

The value of R_{lim} should be such that the active power transferred by the faulted line gets sufficiently dissipated. Hence, P_{lim} is determined as follows:

$$P_{lim} = R_{lim} I_{lim}^2 = \frac{P}{2} \tag{9}$$

After fault clearance, C_{lim} should generate the reactive power needed by the DFIG based power system. This reactive power Q_{lim} is first found as follows [30]:

$$Q_{lim} = C_{lim} \omega V_{lim}^2 = \frac{I_{lim}^2}{\omega C_{lim}} = Q \tag{10}$$

The calculation of apparent power in the limiting impedance branch (S_{lim}) is done as follows:

$$S_{lim} = V_{pcc} I_{lim} = \sqrt{\frac{P^2}{2} + Q^2} \tag{11}$$

So,

$$I_{lim} = \frac{S_{lim}}{V_{pcc}} \tag{12}$$

$$R_{lim} = \frac{V_{PCC}^2 P}{\frac{P^2}{2} + 2Q^2} \tag{13}$$

$$C_{lim} = \frac{\frac{P^2}{4} + Q^2}{V_{PCC}^2 Q \omega} \tag{14}$$

With the use of the above equations the value of R_{lim} is found to be 20Ω and C_{lim} is found as 54μF. The series combination of these elements gives the appropriate limiting impedance for CR-BFCL.

V. LR-BFCL Configuration and Control

In order to see the proficiency of CR-BFCL, it is compared with the previously introduced LR-BFCL [31]. The basic configuration of LR-BFCL is given in Fig. 4. The bridge structure and working principle of LR-BFCL are similar to CR-BFCL. The only difference is that it offers inductive-resistive limiting impedance to the fault current. The same controller can be used to control the switching operation of LR-BFCL as given in Fig. 3. The performance of both of the BFCLs is observed under various fault conditions. The parameters of CR-BFCL and LR-BFCL are given in Table II in the appendix.

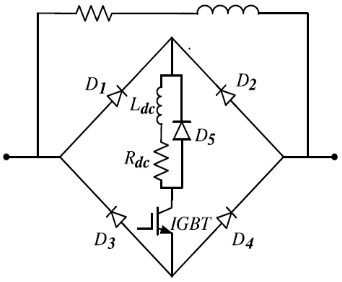

Fig. 4. Schematic Diagram of LR-BFCL

VI. Simulation Considerations

The simulations for all cases are carried out in different scenarios along with some assumptions. The wind speed is assumed constantly to be at 15 m/s as the nature of the wind speed changes the operating points of the wind turbine. At the first the system in Fig. 1 is operated in normal conditions with the DFIG generating rated output. The simulation is carried out for 1s in which the system initializes and settles properly. To check the transient behavior of the model temporary 3LG fault is applied at 0.5s and removed at 0.7s. Circuit breakers situated on the faulted line open at 0.6s and reclose back at 0.9s. The simulation time step which is used for analysis is kept 50μs. The system is simulated and the results are shown for a 3LG fault which is considered as a most severe fault. The parameters used to see the FRT performance of CR-BFCL are voltage at PCC (pu), stator current (pu), output power (MW), consumed reactive power (MVAR), DC link voltage (V) and rotor speed (pu). The results can be clearly observed from the provided plots.

Three cases are considered and simulated for the comparative study of the system behavior:

Case A: Without any FCL

Case B: Using LR-BFCL

Case C: Using CR-BFCL

A. *FRT performance analysis for 3LG fault*

The performance of the aforementioned system subjected to 3LG fault is given in Fig. 5 and Fig. 6. The voltage profile at the PCC, stator current and output power in Fig. 5 show that LR-BFCL elevates the grid voltage to a good extent whereas it is best improved by CR-BFCL. This can also be said for the sudden incremental rise in stator current which needs to be suppressed for stable operation of DFIGs. The fault current is best limited by CR-BFCL and therefore, it can be declared that CR-BFCL is better than LR-BFCL considering the higher and faster voltage recovery operation during a fault. In the absence of any device, the active power of the wind farm goes very low. Both LR-BFCL and CR-BFCL can prevent that from happening but CR- BFCL shows the minimum amount of sag during fault bringing the output to its normal value.

From Fig. 6 it can be seen that reactive power demand at the instant of fault clearance is easily diminished with the use of LR-BFCL and with CR-BFCL, it is the lowest of all. Correspondingly, the DC link voltage rises sharply when no devices are used whereas it is controlled and kept within the nominal value with slight oscillations. The speed response of DFIG can also be seen during fault conditions.

The rotor speed rises during fault due to the difference in the power demand at the time of fault and the generated power from the wind. This can be dangerous for the electromechanical turbine-generator system. A sudden ride is seen in the rotational speed at the fault instant when no controller is applied and also long time is required to get back to the pre-fault value of speed. The rotor speed acceleration is seen to be controlled well with the use of LR-BFCL and best with the use of CR-BFCL.

The plots of voltage and fault current show that by using the proposed devices, we can achieve a fast fault ride-through of DFIG based wind farms. This enhances their transient stability response and the enitire power system is saved from failure.

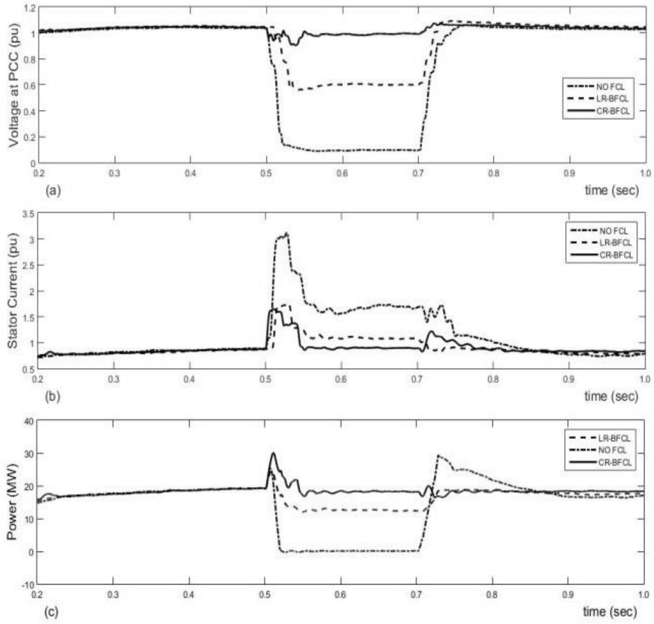

Fig. 5. DFIG response under 3-LG fault in all cases (a) Voltage at PCC, (b) Stator Current, (c) Active Power

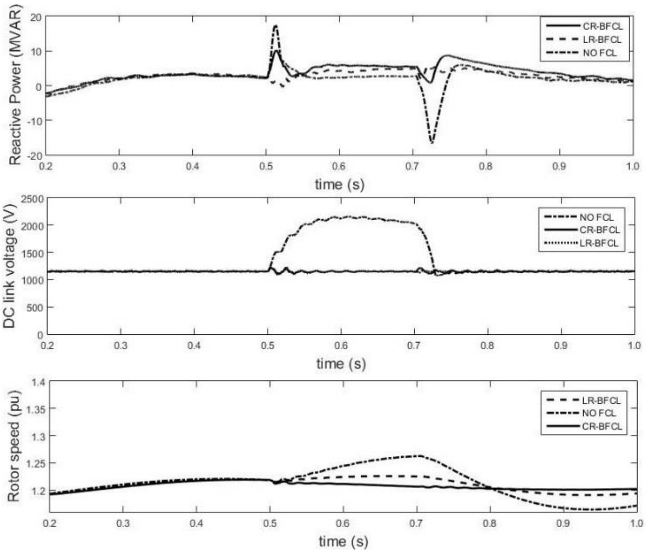

Fig. 6. DFIG response under 3-LG fault in all cases (a) Reactive Power, (b) DC link voltage, (c) Rotor Speed

VII. CONCLUSIONS

From the above simulations it is verified that with the use of BFCL protective circuit, the FRT capability of DFIG gets improved. Two topologies of BFCLs were implemented in the original grid-connected Simulink model of DFIG based wind turbine and it is seen that not only the low voltage ride-through operation of DFIG is achieved but also the reactive power absorption from the grid is minimized. The speed of action of BFCLs is high and therefore grid recovery during fault conditions becomes fast.

Also it is observed that the performance of CR-BFCL is better than that of LR-BFCL. It can be seen LR-BFCL action starts a bit later than CR-BFCL but transients introduced in the system are less. The absorption of reactive power is efficiently decreased with the use of LR-BFCL and gets further minimized with the use of CR-BFCL. It is seen that CR-BFCL not only provides reactive power support but also injects reactive power into the grid. The use of CR-BFCL prevents rotor speed acceleration at the time of grid fault as seen from the results.

VIII. APPENDIX

TABLE I. PARAMETERS OF THE DFIG

Rated Output (P)	2MW
Rated Voltage (V)	690 V
Rated frequency	50 Hz
Stator resistance (R_s)	0.023 pu
Stator inductance (L_s)	0.18 pu (referred to stator)
Stator to rotor turns ratio	0.3
Rotor resistance (R_r)	0.016 pu
Rotor inductance (L_r)	0.16 pu (referred to stator)
Inertia Constant (H)	0.685 s
Mutual inductance (L_m)	2.9 pu

TABLE II. PARAMETERS OF THE DFIG

LR-BFCL		CR- BFCL	
R_{sh}	100 Ω	R_{sh}	10 Ω
L_{sh}	0.1168 mH	C_{sh}	54 μF
L_d	0.01 H	L_d	0.01 H
R_d	0.01 Ω	R_d	0.01 Ω

REFERENCES

[1] The Global Wind Energy Council, "The Global Wind Report ", 2017.

[2] R. Kumar, S. Kumar, N. Singh, and V. Agrawal, "SEPIC converter with 3-level NPC multi-level inverter for wind energy system (WES)," 4th International Conference on Power, Control & Embedded Systems, Allahabad, pp. 1-6, 2017.

[3] R. Kumar, S. Kumar and N. Singh, “Comparative Study of PWM Rectifier and Diode Rectifier –Fed SEPIC Converter for Wind Energy Conversion System," Challenges in Sustainable Development from Energy & Environment Perspective, At MMMUT Gorakhpur in association with ENEA Italy, Vol. 1, No. 1, pp. 256-265, 2017.

[4] V. Yaramasu, B. Wu, P. C. Sen, S. Kouro and M. Narimani, "High-power wind energy conversion systems: State-of-the-art and emerging technologies," in Proceedings of the IEEE, Vol. 103, No. 5, pp. 740-788, 2015.

[5] I. Dincer, ‘‘Renewable energy and sustainable development: A crucial review,’’ J. Renew. Sustain. Energy Rev., Vol. 4, No. 2, pp. 157–175, 2000.

[6] O. Noureldeem , “Behavior of DFIG wind turbines with crowbar protection under short circuit,” Int. J. Electr. Comput. Sci.; Vol. 12, No. 3, pp. 32–37, 2012.

[7] J. Yao, H. Li, Y. Liao, and Z. Chen, “An improved control strategy of limiting the dc-link voltage fluctuation for a doubly fed induction wind generator,” IEEE Trans Power Electron.; Vol. 23, No. 3, pp. 1205–1213, 2008.

[8] G. Pannel, B. Zahawi, D.J. Atkinson, and P. Missailidis, “Evaluation of the performance of a dc-link brake chopper as a DFIG low-voltage fault-ride-through device,” IEEE Trans Energy Convers.; Vol. 28, No. 3, pp. 535–542, 2013.

[9] J. Yang, J.E. Fletcher, and J. O'Relly, “A series-dynamic-resistor-based converter protection scheme for doubly-fed induction generator during various fault conditions,” IEEE Trans Energy Convers.; Vol. 25, No. 2, pp. 422–432, 2010.

[10] A. Causebrook, D. J. Atkinson, and A. G. Jack, “Fault ride-through of large wind farms using series dynamic braking resistors,” IEEE Trans. Power Syst., Vol. 22, pp. 966–975, 2007.

[11] L. Wang, J.Y. Yu, and Y.T. Chen, “Dynamic stability improvement of an integrated offshore wind and marine-current farm using a flywheel

energy-storage system," IET Renew. Power Gener.; Vol. 5, pp.387–396, 2011.
[12] A. M. S. Yunus, M. A. S. Masoum, and A. Abu-Siada, "Application of SMES to enhance the dynamic performance of DFIG during voltage sag and swell," IEEE Trans. Appl. Supercond., Vol. 22, pp. 5702009, 2012.
[13] L. Wang and D.N. Truong, "Stability enhancement of DFIG-based offshore wind farm fed to a multi-machine system using a STATCOM," IEEE Trans. Power Syst., Vol. 28, No. 3, pp. 2882–2889, 2013.
[14] B. Sushabhan, "Application of Unified Power Flow Controller in DFIG Based Wind Turbine," International Journal of Science and Research Vol. 3, No. 6, pp. 748-748, 2014.
[15] S. Xiao, G. Yang, H. Zhou, and H. Geng, "An LVRT Control Strategy Based on Flux Linkage Tracking for DFIG-Based WECS," IEEE Transactions on Industrial Electronics., Vol. 60, No. 7, pp. 2820-2832, 2013.
[16] M. Benbouzid, B. Beltran, Y. Amirat, G. Yao, and H. Mangel, "Second-order sliding mode control for DFIG-based wind turbines fault ride-through capability enhancement", ISA Transactions, Vol. 53, No. 3, pp. 827-833, 2014.
[17] M. J. Morshed, A. Fekih, "A new fault ride-through control for DFIG-based wind energy systems," Electric Power Systems Research, Vol. 146, pp. 258-269, 2017.
[18] N.G. Hingorani, L. Gyugyi, "Understanding FACTS: concepts and technology of flexible AC transmission systems," Wiley-IEEE Press, 2000.
[19] K. E. Okedu; S. M. Muyeen; R. Takahashi, and J. Tamura, "Conceptual Design and Evaluation of a Resistive-Type SFCL for Efficient Fault Ride Through in a DFIG," IEEE Transactions on Applied Superconductivity, Vol. 26, No. 1, 2016.
[20] G. Rashid and M. H. Ali, "Transient Stability Enhancement of Double Fed Induction Machine Based Wind Generator by Bridge-Type Fault Current Limiter," IEEE Transactions on Energy Conversion, Vol. 30, No. 3, 2015.
[21] G. Rashid, and M. H. Ali, "Nonlinear Control-Based Modified BFCL for LVRT Capacity Enhancement of DFIG Based Wind Farm," IEEE Transactions on Energy Conversion, No. 99, 2016.
[22] L. Ye and L. Z. Lin, "Study of Superconducting Fault Current Limiters for System Integration of Wind Farms," IEEE Transactions on Applied Superconductivity, Vol. 20, No. 3, pp. 1233-1237, 2010.
[23] S. Falahzadeh and H. Heydari, "Study of RSFCL effect to improve the behavior of DFIG during a fault," in Proc. 2nd ICREDG, Tehran, Iran, pp. 86–91, 2012.
[24] Z. Zou, X. Xiao, Y. Liu, Y. Zhang and Y. Wang, "Integrated Protection of DFIG-Based Wind Turbine With a Resistive-Type SFCL Under Symmetrical and Asymmetrical Faults," IEEE Transactions on Applied Superconductivity, Vol. 26, No. 7, pp. 1-5, 2016.
[25] S. Alaraifi, A. Moawwad, M. Sh. El Moursi, and V. Khadkikar, "Voltage Booster Schemes for Fault Ride-Through Enhancement of Variable Speed Wind Turbines," IEEE Transactions on Sustainable Energy, Vol. 4, No. 4, pp. 1071–1081, 2013.
[26] Y. Salami, M Firouzi, "Dynamic performance of wind farms with bridge-type superconducting fault current limiter in distribution grid," 2nd International Conference on Electric Power and Energy Conversion Systems, Sharjah, IEEE, 2011.
[27] M. Firouzi and G. B. Gharehpetian, "Improving Fault Ride-Through Capability of Fixed-Speed Wind Turbine by Using Bridge-Type Fault Current Limiter," IEEE Transactions on Energy Conversion, Vol. 28, No. 2, pp. 361–369, 2013.
[28] P. M. Anderson and Anjan Bose, "Stability Simulation of Wind Turbine Systems," IEEE Transactions on Power Apparatus and Systems, Vol. PAS-102, No.12, pp. 3791-3795, 1983.
[29] A. Petersson, "Analysis, modeling, and control of doubly-fed induction generators for wind turbines," Ph.D. thesis, Göteborg, Sweden, 2003.
[30] E.J. Bueno, S. CÓbreces, F. J. RodrÍguez, Á. HernÁndez, F. Espinosa, "Design of a back-to-back NPC converter interface for wind turbines with squirrel-cage induction generator," IEEE Transactions on Energy conversion, Vol. 23, No. 3, pp. 932-945, 2008.
[31] G. Rashid and M. H. Ali, "Transient Stability Enhancement of Double Fed Induction Machine Based Wind Generator by Bridge-Type Fault Current Limiter," IEEE Transactions on Energy Conversion, Vol. 30, No. 3, 2015.